

Rapid carrier relaxation in $\text{In}_{0.4}\text{Ga}_{0.6}\text{As}/\text{GaAs}$ quantum dots characterized by differential transmission spectroscopy

T. S. Sosnowski and T. B. Norris

Center for Ultrafast Optical Science and Department of Electrical Engineering and Computer Science, University of Michigan, Ann Arbor, Michigan 48109-2099

H. Jiang, J. Singh, K. Kamath, and P. Bhattacharya

Solid State Electronics Laboratory and Department of Electrical Engineering and Computer Science, University of Michigan, Ann Arbor, Michigan 48109-2099

(Received 24 February 1998)

Carrier relaxation in self-organized $\text{In}_{0.4}\text{Ga}_{0.6}\text{As}/\text{GaAs}$ quantum dots is investigated by time-resolved differential transmission measurements. The dots have a base dimension of around 14 nm and a height of 7 nm, leading to an average energy separation of the ground and first excited electronic states much greater than the LO-phonon energy, so the phonon-mediated electron relaxation is expected to be slow. Our measurements indicate that, even at low carrier densities (less than one electron-hole pair per dot), the electron and hole relaxation time constants are 5.2 and 0.6 ps, respectively; this indicates a lack of any “phonon bottleneck” and is consistent with a model of electrons scattering from holes which can relax rapidly via phonon emission. [S0163-1829(98)52716-6]

In recent research on low-dimensional semiconductor structures, quantum dots have been attracting much attention due to the physical effects observed in quasi-zero-dimensional systems and for their potential device applications. Technologically, quantum dots are expected to be especially important for interband and inter-sub-band semiconductor lasers where their δ -function-like density of states will result in very large differential gains and temperature insensitivity,¹ and for new types of infrared detectors. Discovery of the self-organization of quantum dots during high-strain epitaxial growth has enabled practical quantum dot devices,²⁻⁴ including quantum dot lasers.⁵⁻⁷ Of particular importance for both types of devices is the physics of carrier relaxation in the dots, and specifically the possibility of a “phonon bottleneck” that is expected to drastically slow carrier relaxation in small dots.^{8,9} This bottleneck is detrimental for quantum dot lasers because it can limit their maximum modulation bandwidth; on the other hand quantum dot detectors rely on it for low-noise performance.

In this investigation we study carrier relaxation under low-carrier-density conditions in self-organized $\text{In}_{0.4}\text{Ga}_{0.6}\text{As}/\text{GaAs}$ quantum dots by means of differential transmission (DT) measurements. We directly time resolve the relaxation from the GaAs region to the ground state and the relaxation from the first excited state to the ground state. Although other groups have reported differential transmission measurements on very different systems such as *II-VI* quantum dots,¹⁰ studies reporting on carrier relaxation in *III-V* self-organized quantum dot systems have relied on cw or time-resolved photoluminescence (PL) techniques that generally have insufficient time resolution for relaxation on the time scales we observe and are also indirect measurements of carrier level occupation.¹¹⁻¹⁴

The sample considered in this report was grown by molecular-beam epitaxy and consisted of four layers of $\text{In}_{0.4}\text{Ga}_{0.6}\text{As}$ quantum dots in the center of a 0.2- μm -thick

GaAs layer with 1 μm $\text{Al}_{0.3}\text{Ga}_{0.7}\text{As}$ carrier confinement layers above and below the GaAs. The $\text{In}_x\text{Ga}_{1-x}\text{As}$ was grown at 520 °C at a rate of 0.25 ML per second while the rest of the sample was grown at 620 °C at 0.2 nm per second. The initial dot layer consists of 7 ML of $\text{In}_x\text{Ga}_{1-x}\text{As}$, while additional dot layers contain only 5 ML.¹⁵ The dot layers are separated by 2.5-nm-thick GaAs barriers. This structure closely resembles the quantum dot laser structure grown by Kamath *et al.* except it is undoped.⁶ Cross-sectional transmission electron microscopy reveals that the dots have a pyramidal shape¹⁵ with a base width of 14 nm and a height of 7 nm. Atomic-force microscopy reveals a dot density (per layer) of $5 \times 10^{10} \text{ cm}^{-2}$. Additional discussion of the characterization of similar samples is given in Ref. 15. The sample was antireflection coated (to eliminate Fabry-Perot effects on the optical spectrum), mounted on sapphire, and the GaAs substrate was removed by selective etching to eliminate any possible contribution of the substrate to the optical spectra. The sample was held at 10 K.

An eight-band $\mathbf{k} \cdot \mathbf{p}$ model including the strain distribution in the dots (described in detail in Ref. 16) predicts the band structure shown in Fig. 1. There are two electron levels confined in the dots. There are a large number of closely spaced hole states in the dots; only the ground state and the first three excited states are shown. The interband optical-matrix element is calculated to be strong only between electron and hole levels with the same quantum number; thus the absorption and PL spectra will be dominated by transitions at 1.248 eV (which we label *E1H1*) and 1.33 eV (*E2H2*). PL measurements made with an 800-nm 85-fs pulsed excitation source at 10 K are shown in Fig. 2 for different excitation densities and clearly show the existence of two transitions corresponding to the two confined electronic levels. The peak at low excitation densities at 980 nm (1.265 eV) corresponds to *E1H1* emission and its width is due to inhomoge-

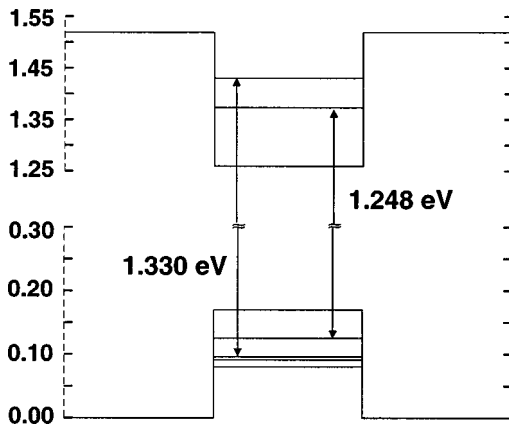


FIG. 1. Calculated electronic spectrum for an $\text{In}_{0.4}/\text{Ga}_{0.6}\text{As}$ dot with base width 14.5 nm and height 7.3 nm and 7 ML wetting layer. Biaxial strain is assumed in the entire dot area.

neous broadening from a distribution in dot sizes. With higher excitation the ground state fills up and luminescence corresponding to the $E2H2$ transition at 925 nm (1.34 eV) is also observable. These transition energies are in reasonable agreement with the calculated values given the uncertainties in the exact dot parameters. Time-resolved PL measurements on similar samples reveal a ground-state luminescence lifetime of ~ 700 ps that is essentially insensitive to the number of dot layers in the sample.¹⁵

Differential transmission experiments were performed using a 250-kHz Ti:sapphire regenerative amplifier which produces 85-fs 4- μJ pulses at 800 nm.¹⁷ The output was split into two and the first beam generated a single-filament white light continuum. The probe pulse, with a spectrum extending from 900 to 1100 nm, was obtained by filtering the continuum with a Schott Glass Technologies RG1000 filter. For experiments requiring a 920-nm pump pulse, a continuum was generated with the second beam as well and filtered with a 10-nm bandwidth 920-nm interference filter; for experiments requiring an 800-nm pump pulse the second beam was simply attenuated. The pump beam was mechanically chopped at 2 kHz and lock-in detection of the probe beam

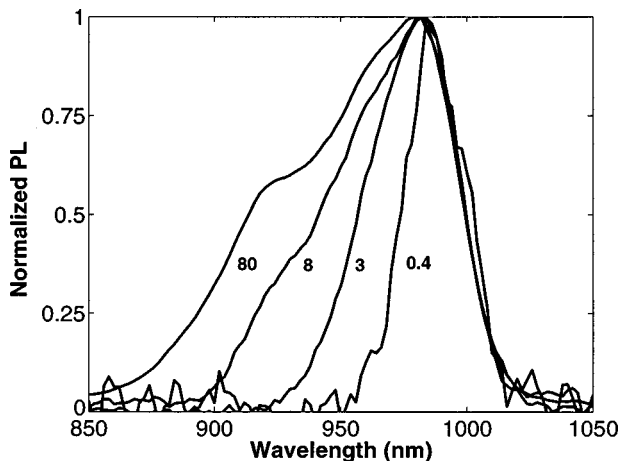


FIG. 2. PL measurements at 10 K are shown for the four-layer $\text{In}_{0.4}\text{Ga}_{0.6}\text{As}$ quantum dot sample. The estimated number of carriers per dot injected into the GaAs barrier region is shown next to each curve. The total dot density is $2 \times 10^{11} \text{ cm}^{-2}$.

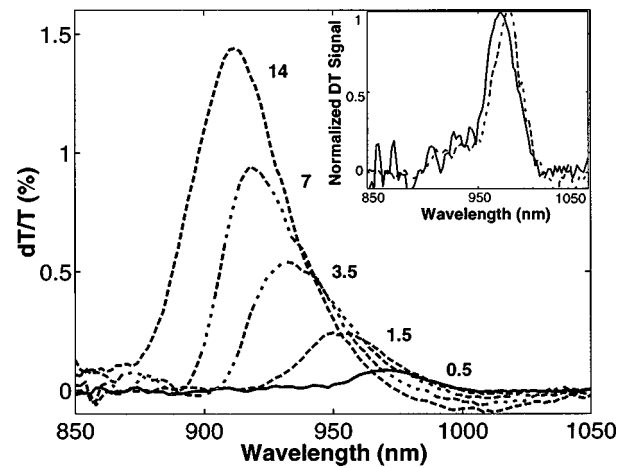


FIG. 3. The differential transmission is plotted vs wavelength for the probe pulse delayed 67 ps from the pump pulse. The estimated carrier density scaled to the dot density (i.e., the effective number of electrons per dot injected into the GaAs region) is indicated for each curve. The inset shows normalized DT signals for carrier densities much less than 1 per dot for an 800-nm pump (solid line) and a 920-nm pump (dashed line).

was used to measure the DT signal. The transmitted probe spectrum was measured with ~ 1 -nm resolution. We used DT measurements to characterize the carrier dynamics because at low densities the signal is directly related to changes in the occupation of the dot levels, $[\Delta T(\hbar\omega)]/T(\hbar\omega) = (f_e + f_h)\alpha_0(\hbar\omega)$, where f_e (f_h) are the electron (hole) occupation probabilities and $\alpha_0(\hbar\omega)$ is the unexcited absorption coefficient of the quantum dots. On the other hand, luminescence measurements are sensitive to the occupation of dot levels only through the product $f_e f_h$.

Figure 3 shows DT signals measured for a range of injected carrier densities when the probe pulse is delayed 67 ps from the 800-nm pump pulse. For carrier densities much above one electron-hole pair for every two dots the signals do not appear to reflect the energy levels observable from the PL in an obvious way. In fact the signal is negative at the long-wavelength end of the spectrum indicating induced absorption. At present we are unable to explain the high-density spectrum including apparent level shifts. At low carrier densities, however, the DT signal matches well with the PL as shown in the inset of Fig. 3. Also shown in the inset is the differential transmission spectrum for a 920-nm pump pulse (corresponding to the $E2H2$ transition), and it also matches well with the PL. We therefore limit ourselves in the remainder of this paper to a discussion of the low-carrier-density regime, where the DT spectrum can be interpreted simply in terms of dot level populations.

Figure 4 shows DT signals measured using a 10-nm bandwidth pump pulse centered at 920 nm and probe wavelengths of 980 and 923 nm, corresponding to the $E1H1$ and $E2H2$ transitions. The pump pulse produced an estimated carrier density of 10^{10} cm^{-2} in the $n=2$ state, corresponding to one electron-hole pair for every 20 dots. These measurements show that the injected carriers leave the $n=2$ states (the decay of the 923-nm signal) with the same time constants as they arrive at the $n=1$ states (the risetime of the 980-nm signal). The inset of this figure plots a flipped version of the 923-nm signal on top of the 980-nm signal to illustrate the

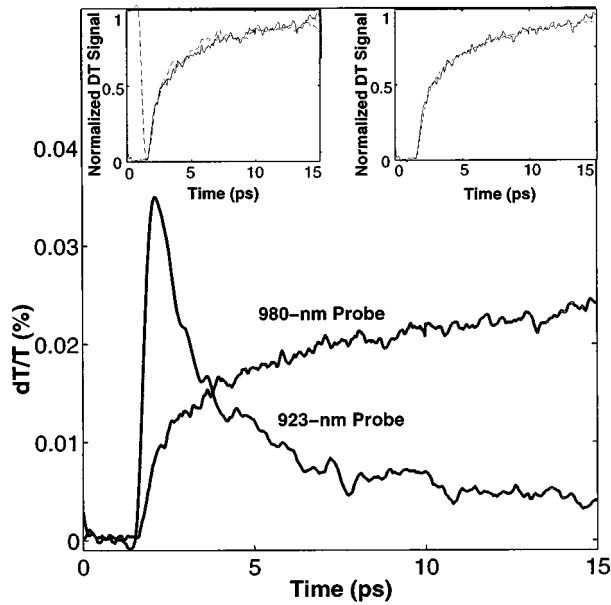


FIG. 4. DT signals measured with a 920-nm pump and a 923-nm or 980-nm probe are plotted as a function of time. The left inset shows a flipped version of the 923-nm probe signal plotted with the 980-nm signal to emphasize the similarity. The right inset shows a curve fitting for the 920-nm pump 980-nm probe signal fit by signal $\propto 1 - 0.5e^{-t/0.62} - 0.5e^{-t/5.2}$.

excellent agreement. We therefore believe we have an accurate measurement of the $n=2$ state to the $n=1$ state relaxation time (τ_{21}). Because the electron and hole $n=1$ states contribute equally to the DT spectrum at 980 nm, we fit the dynamics with two exponential components of equal weight. An excellent fit is obtained for time constants of 0.6 and 5.2 ps as can be seen in the right inset of Fig. 4. As the phonon-mediated hole relaxation rate is expected to be relatively fast in this and similar quantum dot systems, we attribute the fast component to hole relaxation. The longer time constant of 5.2 ps, however, would be surprisingly short for phonon-mediated relaxation between the electron $n=2$ and $n=1$ levels, considering that the separation of the electronic levels (58 meV average) is much larger than the LO phonon energy of 30 meV. It is possible that some of the dots in the inhomogeneous distribution may have electronic levels which can relax via resonant two LO-phonon emission. A two phonon transition could not explain the results, however, because it is a highly resonant transition and would occur only for a very narrow range of dot sizes,¹⁸ and not for the entire distribution. Auger-type scattering processes mentioned in other reports,^{11,19} such as scattering of an electron in the quantum dot with an electron in the GaAs barrier, cannot occur at the carrier densities in these measurements. Electron-hole scattering involving discrete dot states might naively be ruled out as a possible relaxation mechanism, as it would be difficult to satisfy strict energy conservation in the scattering process. However, if we include the nonzero linewidth of the hole levels due to hole-phonon scattering, the strict energy conservation requirement is relaxed, and electron-hole scattering can provide an efficient channel for the electron to lose energy.^{18,20} Figure 5 shows the calculated electron-hole scattering time as a function of the hole relaxation time using the model given in Refs. 18 and 20 for our

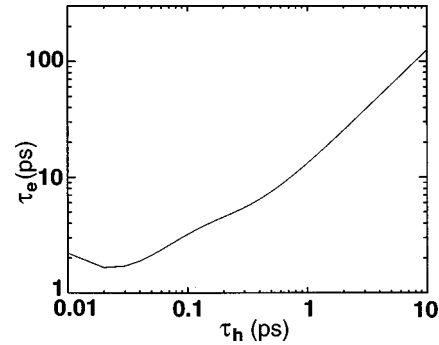


FIG. 5. Level-2-electron's lifetime dependence on the lifetime of holes due to electron-hole scattering.

quantum dot system with one electron-hole pair per dot. Taking the 0.6-ps time constant observed in the 980-nm-probe signal as indicative of the hole relaxation time and assuming this is close to the average lifetime of the hole states in the dot, we expect from Fig. 5 an electron relaxation time of around 8 ps. This is reasonably consistent with our observed value of 5.2 ps.

Having determined the electron and hole $n=2$ to $n=1$ relaxation rates, we then applied the DT technique to measure the capture rate of carriers from the GaAs barrier region into the dots. Figure 6 shows the normalized DT signals measured with an 800-nm pump pulse at probe wavelengths of 980 and 925 nm. The pump pulse injected carriers into the GaAs barrier region at an estimated density of 10^{11} cm^{-2} . The 925-nm-probe signal is fit reasonably by a rate equation modeling the barrier to $n=2$ state relaxation time (τ_{b2}) as 2.8 ps and τ_{21} as 5.2 ps as measured above. This rate equation model also fits the rise of the dot ground-state population (980-nm-probe signal) quite well, although we should note that the 980-nm signal can also be fit simply by a single exponential with an 8-ps time constant. It is not clear why separate hole and electron relaxation times are not observable for the 800-nm pump 980-nm probe signal, although it does seem that the present signal-to-noise ratio is insufficient for a rate equation fitting procedure to be sensitive enough to

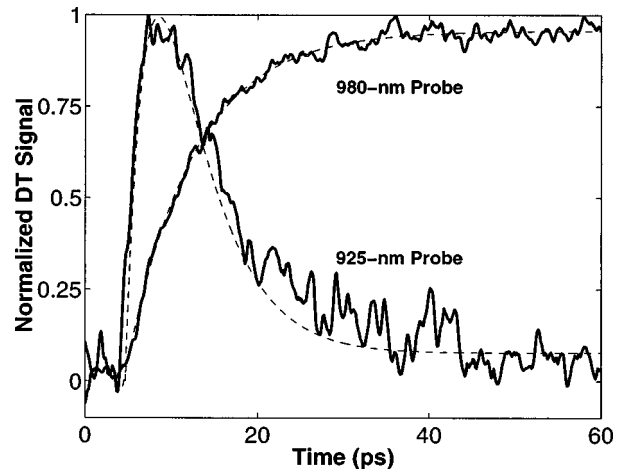


FIG. 6. DT signals (solid lines) measured with a 800-nm pump and a 925-nm or 980-nm probe are plotted as a function of time. Rate equation curve fits, as described in the text, are shown as dashed lines.

determine if there are multiple time constants for either the 925- or 980-nm probe signals. In any case it is clear that both carriers relax to the $n=1$ state within 8 ps.

In summary, we have used femtosecond differential transmission measurements to time resolve the $n=2$ to $n=1$ relaxation and the GaAs barrier to $n=2$ relaxation for $\text{In}_{0.4}\text{Ga}_{0.6}\text{As}/\text{GaAs}$ self-organized quantum dots at low carrier densities. Direct photoinjection of carriers into the $n=2$ states reveals that τ_{21} for holes is 0.6 ps. τ_{21} for electrons is found to be 5.2 ps, which is much more rapid than expected for the electrons and indicates the phonon bottleneck is not effective for this system. The observed time constants are consistent with a model for electron relaxation via electron-hole scattering, where the scattered holes can rapidly lose their excess energy through phonon emission. When carriers are photoinjected into the GaAs barrier region, relaxation into the $n=2$ and $n=1$ states of the dot occurs with time constants of 2.8 and 8 ps, respectively. The latter relaxation times are also extremely rapid, and further mod-

eling is needed to completely characterize this relaxation pathway. The rapid relaxations observed in this work indicate that interband lasers made from these structures may have maximum modulation rates comparable to those of quantum-well lasers, for which the carrier capture times are typically 1–10 ps, although the dynamics observed in high-density experiments remain to be correlated with the observed laser modulation bandwidths. On the other hand, far infrared or midinfrared lasers and detectors that operate purely on intersubband electronic transitions (and which require long excited state lifetimes) may still have a very long τ_{21} since the hole concentration in such devices is essentially zero. Measurements of relaxation in unipolar structures remain to be done.

This work was supported by ARO Grant No. DAAH04-96-1-0414 and the NSF through the Center for Ultrafast Optical Science.

-
- ¹Y. Arakawa and A. Yariv, *IEEE J. Quantum Electron.* **QE-22**, 1887 (1986).
- ²P. R. Berger, K. Chang, P. Bhattacharya, J. Singh, and K. K. Bajaj, *Appl. Phys. Lett.* **53**, 684 (1988).
- ³O. Brandt, L. Tapfer, K. Ploog, R. Bierwolf, M. Hohenstein, F. Phillip, H. Lage, and A. Heberle, *Phys. Rev. B* **44**, 8043 (1991).
- ⁴D. Leonard, M. Krishnamurthy, C. M. Reaves, S. P. Denbaars, and P. M. Petroff, *Appl. Phys. Lett.* **63**, 3202 (1993).
- ⁵N. Kirstaedter *et al.*, *Appl. Phys. Lett.* **69**, 1226 (1996).
- ⁶K. Kamath, P. Bhattacharya, T. Sosnowski, T. Norris, and J. Phillips, *Electron. Lett.* **32**, 1374 (1996).
- ⁷H. Saito, K. Nishi, I. Ogura, S. Sugou, and Y. Sugimoto, *Appl. Phys. Lett.* **69**, 3140 (1996).
- ⁸H. Bensity, C. M. Sotomayor-Torres, and C. Weisbuch, *Phys. Rev. B* **44**, 10 945 (1991).
- ⁹U. Bockelmann and G. Bastard, *Phys. Rev. B* **42**, 8947 (1990).
- ¹⁰U. Woggon, H. Giessen, F. Gindele, O. Wind, B. Fluegel, and N. Peyghambarian, *Phys. Rev. B* **54**, 17 681 (1996).
- ¹¹B. Ohnesorge, M. Albrecht, J. Oshinowo, A. Forchel, and Y. Arakawa, *Phys. Rev. B* **54**, 11 532 (1996).
- ¹²M. J. Steer *et al.*, *Phys. Rev. B* **54**, 17 738 (1996).
- ¹³K. H. Schmidt, G. Medeiros-Ribeiro, M. Oestreich, P. M. Petroff, and G. H. Dohler, *Phys. Rev. B* **54**, 11 346 (1996).
- ¹⁴S. Raymond *et al.*, *Phys. Rev. B* **54**, 11 548 (1996).
- ¹⁵K. Kamath *et al.*, *Appl. Phys. Lett.* **71**, 927 (1997).
- ¹⁶H. Jiang and J. Singh, *Phys. Rev. B* **56**, 4696 (1997).
- ¹⁷J.-K. Rhee, T. S. Sosnowski, T. B. Norris, J. A. Arns, and W. S. Colburn, *Opt. Lett.* **19**, 1550 (1994).
- ¹⁸H. Jiang and J. Singh, *Physica E* (to be published).
- ¹⁹Al. L. Efros, V. A. Kharchenko, and M. Rosen, *Solid State Commun.* **93**, 281 (1995).
- ²⁰I. Vurgaftman and J. Singh, *Appl. Phys. Lett.* **64**, 232 (1994).